Photonic crystal biosensor based on angular spectrum analysis

Elewout Hallynck* and Peter Bienstman

Photonics Research Group, Department of Information Technology, Ghent University - imec, Sint-Pietersnieuwstraat 41, 9000 Gent, Belgium

**elewout.hallynck@intec.ugent.be*

Abstract: The need for cost effective and reliable biosensors in e.g. medical applications is an ever growing and everlasting one. Not only do we strive to increase sensitivity and detection limit of such sensors; ease of fabrication or implementation are equally important. In this work, we propose a novel, photonic crystal based biosensor that is able to operate at a single frequency, contrary to resonance based sensors. In a certain frequency range, guided photonic crystal modes can couple to free space modes resulting in a Lorentzian shape in the angular spectrum. This Lorentzian can shift due to refractive index changes and simulations have shown sensitivities of 65° per refractive index unit and more.

OCIS codes: (050.5298) Photonic crystals; (070.4790) Spectrum analysis; (130.6010) Sensors; (280.1415) Biological sensing and sensors.

References and links

1. M. Huang, A. A. Yanik, T.-Y. Chang, and H. Altug, "Sub-wavelength nanofluidics in photonic crystal sensors," Opt. Express **17**, 24224–24233 (2009).
2. A. Densmore, M. Vachon, D.-X. Xu, S. Janz, R. Ma, Y.-H. Li, G. Lopinski, A. Delâge, J. Lapointe, C. C. Luebbert, Q. Y. Liu, P. Cheben, and J. H. Schmid, "Silicon photonic wire biosensor array for multiplexed real-time and label-free molecular detection," Opt. Lett. **34**, 3598–3600 (2009).
3. P. Debackere, R. Baets, and P. Bienstman, "Bulk sensing experiments using a surface-plasmon interferometer," Opt. Lett. **34**, 2858–2860 (2009).
4. K. De Vos, J. Girones, T. Claes, Y. De Koninck, S. Popelka, E. Schacht, R. Baets, and P. Bienstman, "Multiplexed antibody detection with an array of silicon-on-insulator microring resonators," IEEE Photon. J. **1**, 225–235 (2009).
5. T. Claes, J. Molera, K. De Vos, E. Schacht, R. Baets, and P. Bienstman, "Label-free biosensing with a slot-waveguide-based ring resonator in silicon on insulator," IEEE Photon. J. **1**, 197–204 (2009).
6. X. Fan, I. M. White, S. I. Shopova, H. Zhu, J. D. Suter, and Y. Sun, "Sensitive optical biosensors for unlabeled targets: A review," Anal. Chim. Acta **620**, 8– 26 (2008).
7. J. D. Joannopoulos, S. G. Johnson, J. N. Winn, and R. D. Meade, *Photonic Crystals: Molding the Flow of Light* (Princeton University Press, 2008), 2nd ed.
8. E. Chow, A. Grot, L. W. Mirkarimi, M. Sigalas, and G. Girolami, "Ultracompact biochemical sensor built with two-dimensional photoniccrystal microcavity," Opt. Lett. **29**, 1093–1095 (2004).
9. S. Xiao, N. A. Mortensen, "Highly dispersive photonic band-gap-edge optofluidic biosensors," J. Europ. Opt. Soc. Rap. Public. **1**, 06026 (2006).
10. J. H. Schmid, W. Sinclair, J. García, S. Janz, J. Lapointe, D. Poitras, Y. Li, T. Mischki, G. Lopinski, P. Cheben, A. Delâge, A. Densmore, P. Waldron, and D.-X. Xu, "Silicon-on-insulator guided mode resonant grating for evanescent field molecular sensing," Opt. Express **17**, 18371–18380 (2009).
11. S. Fan and J. D. Joannopoulos, "Analysis of guided resonances in photonic crystal slabs," Phys. Rev. B **65**, 235112 (2002).
12. A. F. Oskooi, D. Roundy, M. Ibanescu, P. Bermel, J. D. Joannopoulos, and S. G. Johnson, "MEEP: A flexible free-software package for electromagnetic simulations by the FDTD method," Comp. Phys. Commun. **181**, 687–702 (2010).

#128700 - $15.00 USD Received 20 May 2010; revised 12 Jul 2010; accepted 18 Jul 2010; published 9 Aug 2010

13. A. Hessel and A. A. Oliner, "A new theory of wood's anomalies on optical gratings," Appl. Opt. **4**, 1275–1297 (1965).
14. A. A. Yanik, M. Huang, A. Artar, T.-Y. Chang, and H. Altug, "Integrated nanoplasmonic-nanofluidic biosensors with targeted delivery of analytes," Appl. Phys. Lett. **96**, 021101 (2010).
15. N. L. Thomas, R. Houdré, M. V. Kotlyar, D. O'Brien, and T. F. Krauss, "Exploring light propagating in photonic crystals with fourier optics," J. Opt. Soc. Am. B **24**, 2964–2971 (2007).
16. T. Kan, K. Matsumoto, and I. Shimoyama, "Nano-pillar structure for sensitivity enhancement of spr sensor," in "Solid-State Sensors, Actuators and Microsystems Conference, 2009. TRANSDUCERS 2009. International," (2009), pp. 1481–1484.

1. Introduction

Optical biosensing is a research field that, despite already being around for quite a few years, to this day still yields a great deal of scientific output [1–5]. This comes as no surprise as there is and always will be a need for cost effective and reliable biosensors and this in many domains (e.g. medical, food production, military).

There are basically two types of photonics based biosensors: fluorescent based and label-free ones. In a fluorescent based sensing scheme, the molecules that we want to measure need to be labeled with a fluorescent or radioactive marker. When illuminating the molecules, the labels will emit light or a radiowave and depending on the intensity of the captured signal, we can determine the concentration. Although this seems a fairly simple method, the labeling procedure of the biomolecules is quite complicated. An alternative is making use of label-free sensing. In label-free sensing, biomolecules bond with receptor molecules attached to the sensor. Due to this bonding, the refractive index close to the sensing area will change. The change in refractive index is then a measure for the concentration of the biomolecules. Apart from this, label-free sensors can also be used for measuring a bulk refractive index (e.g. when immersing the sensor in water with a certain NaCl concentration).

Quite a few biosensor concepts using photonics have been investigated over the years [6]. Here we present a novel sensing method, based on photonic crystals (PhCs) [7]. There are already several ways to design a PhC biosensor: measuring the shift of a resonance peak induced by a defect in the PhC [8], monitoring the band gap shift [9] or making use of guided resonances [10]. In the first two cases, light is constantly guided in the plane of the PhC, in the latter case, the direction of the incident and outgoing light is out of the PhC plane. In the sensing concept described in this paper, the incident light comes in in the plane of the PhC and is then coupled out of the plane, much like a grating coupler (see Fig. 1).

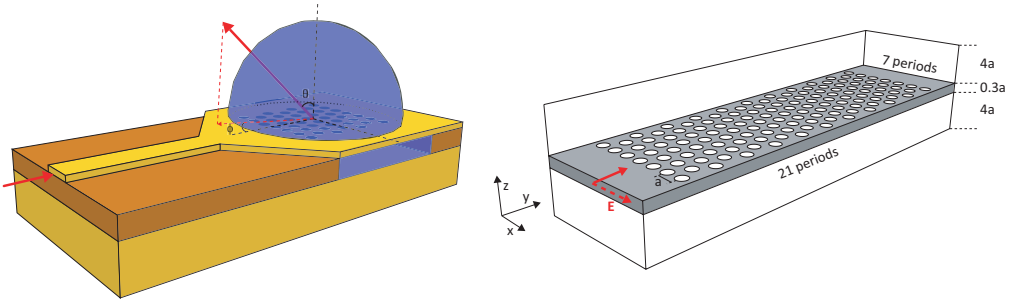

Fig. 1. Light enters the PhC biosensor by means of a waveguide and is coupled to free space as a beam with inclination θ and azimuth ϕ (left). The simulated structure used for FDTD simulations is shown in the right figure. All sizes are normalized to the lattice constant a. The grid resolution used is 56 pixels per unit of distance.

#128700 - $15.00 USD Received 20 May 2010; revised 12 Jul 2010; accepted 18 Jul 2010; published 9 Aug 2010

2. Angular spectrum analysis sensor concept and simulation methods

In photonic crystals there are two types of guided modes: modes above and below the light line. The modes below the light line are true guided modes and possess an infinite lifetime. The other modes (above the light line) are called resonant guided modes [11] and can couple to the continuous spectrum of free space modes. It is the latter type that determines the behaviour of the proposed structure. Figure 2 shows the transmission, reflection and radiated (either upwards or downwards since the structure is symmetric) flux spectra of a $0.3a$ thick bulk silicon PhC slab comprising holes of diameter $0.8a$ in a triangular lattice (where a is the lattice constant), excited with x-polarized light in the ΓM direction (see Fig. 1 (right)). The refractive index in the holes as well as that of the cladding layers above and below the PhC slab is 1.33, the refractive index of water. The resolution is set to 56 pixels per unit of distance. Simulations are carried out using a freely available FDTD method [12]. Note that the sum of the flux spectra does not equal 1 as the flux planes defined in our simulations do not constitute a closed volume (the flux plane for out of plane radiation is located at a relatively large distance from the slab and the flux planes for reflection and transmission only cover the input waveguide).

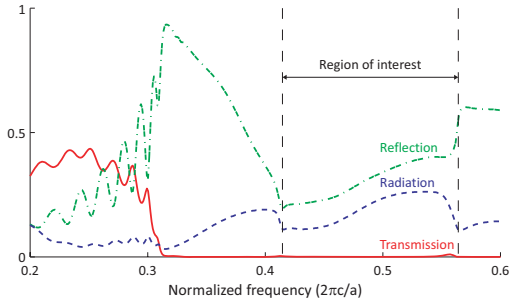

Fig. 2. In a certain frequency region, above the light line, guided modes can couple to free space modes. The fluxes shown in this figure are calculated for a triangular silicon PhC slab with hole diameter $0.8a$, thickness $0.3a$, excited in the ΓM direction. The radiation flux represents either the down- or upward direction since the structure is symmetric.

In Fig. 2 we see a clearly marked frequency region bound by dips in the out of plane radiated flux. In order to determine what exactly is happening in this region, we must examine the fields themselves. Figure 3 shows the calculated angular spectrum of the Poynting vector projected on the vertical direction for a certain frequency in the region of interest.

We can distinguish the Lorentzian shape [13] which we would expect to see due to the resonant coupling of guided modes to free space modes. As with other diffraction gratings, the angle at which a beam with a certain frequency is radiated, is determined by the momentum matching condition. The angular position of the peak shifts not only in function of frequency but also due to changes in refractive index which makes it interesting for sensing applications.

Now that we have qualitatively determined a shift, we can perform a quantitative analysis.

3. Simulation results

There are a lot of parameters that can be tuned when designing this structure. In the following, the results of extensive FDTD simulations are presented for the most important of these parameters: the type of cladding configuration and the direction of light excitation.

#128700 - $15.00 USD Received 20 May 2010; revised 12 Jul 2010; accepted 18 Jul 2010; published 9 Aug 2010

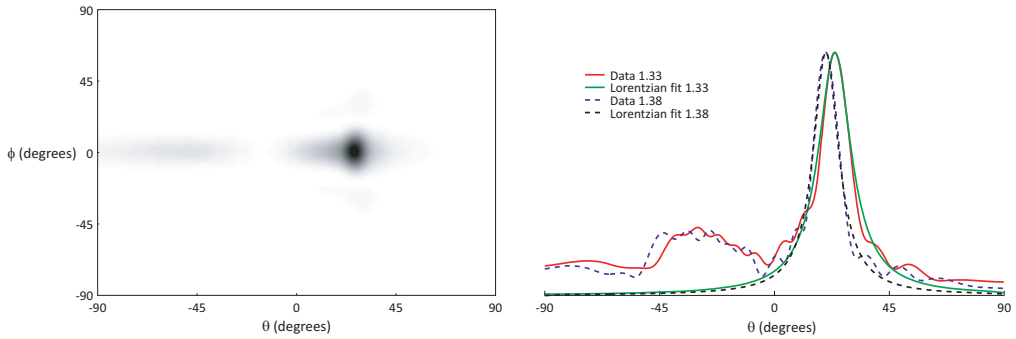

Fig. 3. The angular spectrum (left) and cross-section at ϕ=0° (right) of the vertically projected Poynting vector of the proposed structure with a symmetric cladding (i.e. refractive index above and below PhC slab equals that of the holes) at normalized frequency 0.53488. A Lorentzian resonance shape is clearly visible.

3.1. Different cladding configurations

Depending on fabrication and implementation of microfluidics [1, 14], one can wonder how the situation with respect to the refractive index in the neighbourhood of the PhC membrane will become. Therefore, we have studied the three main situations that can arise: only the refractive index in the PhC holes changes and above and below the membrane, there is air (henceforth called the *no cladding* type), one cladding layer consists of air while the other has the same refractive index as that of the holes (*asymmetric cladding*) or both cladding layers and holes experience a change in refractive index (*symmetric cladding*). For each of these situations, simulations have been carried out for several refractive indices which allows us to determine a shift per refractive index unit (RIU).

There are two ways to see a kind of shift: we can look at the angular spectrum for a fixed frequency by using a spatial Fourier measurement setup [15] or we measure the power for a given angle while scanning the frequency range. Both methods have been investigated and the results for the different cladding configurations are presented in Fig. 4. It should however be noted that the major advantage of the first method is that the light source in a fabricated device only needs to be single frequency.

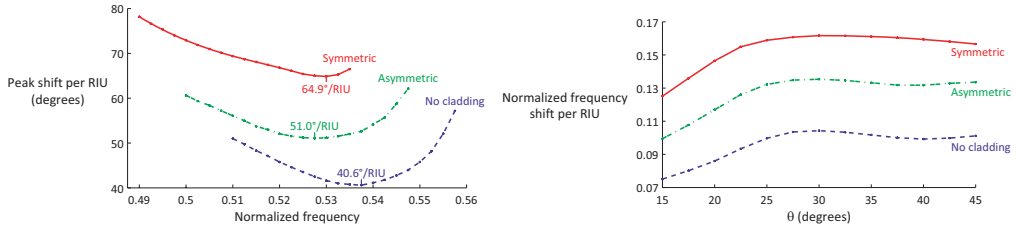

Fig. 4. As expected, the shift for the symmetric cladding configuration is the highest in both approaches (left: monitoring angular shift at a fixed frequency; right: measuring frequency shift at a fixed angle).

Like we would intuitively expect, for both measurement methods, the *symmetric cladding* type is more sensitive than the *asymmetric cladding* configuration which is in turn more sensitive than the *no cladding* type. When measuring using the Fourier setup, it is advised to measure

#128700 - $15.00 USD Received 20 May 2010; revised 12 Jul 2010; accepted 18 Jul 2010; published 9 Aug 2010

at a high frequency because a) the light is coupled out at an angle close to the normal and is therefore easier to capture using a lens and b) as will become apparent in what follows, the width of the resonance peak decreases with increasing frequency.

Using the other measurement method, we see for the three types a gradual increase of sensitivity with increasing angle until it becomes stable at about 25° and onwards.

3.2. *Excitation along the ΓK direction*

Up until now, we have always excited light in the PhC along the ΓM direction. Exciting it along the perpendicular ΓK direction gives a slightly different angular spectrum as shown in Fig. 5.

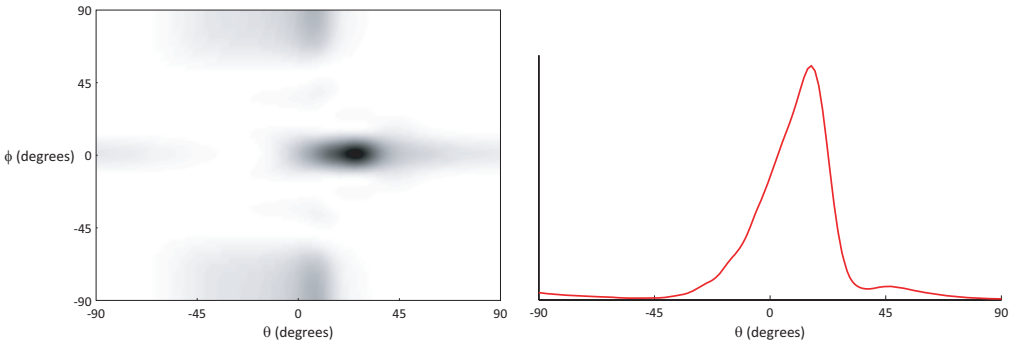

Fig. 5. The angular spectrum at normalized frequency 0.53488 (left) and cross-section at ϕ=0° and normalized frequency 0.569 (right) of the proposed structure with a symmetric cladding. A portion of the light is scattered under an angle ϕ=90° and the Lorentzian shape is distorted (this is more clearly visible in the right figure).

We can see that the Lorentzian shape is distorted (more clearly visible in the right part of Fig. 5) and that now also light is scattered at an angle ϕ=90°.

As it is difficult to fit a proper Lorentzian to the ΓK spectra we can make an estimation of the shift by simply observing the maxima of the peaks. It turns out that the sensitivity is roughly equal to that of the structure excited in the ΓM direction.

3.3. *Other parameters*

It is clear that there are still a lot of other properties that can be optimized (e.g. the shape of the unit cell, slab thickness, polarization of incident light, the periodic lattice). We have investigated the effect of the number of periods in the direction of light propagation but have found that it is of little influence. The hole diameter has been chosen sufficiently large as to maximize the light-matter interaction keeping in mind technological limitations for eventual fabrication of the device (i.e. minimal distance between adjacent holes). The influence of the slab thickness has been investigated briefly and we have found that with decreasing thickness, the frequency region in which the Lorentzian shape appears widens and shifts to higher frequencies and the sensitivity also slightly increases.

3.4. *Noise analysis and detection limit*

In simulations, it is virtually impossible to take into account all noise factors that will influence measurements (e.g. temperature variations, fabrication errors). In order to already make some predictions on how the structure will react due to this noise, we can add Gaussian noise to the simulated signal. By performing a Monte Carlo simulation, i.e. repeatedly determining the

#128700 - $15.00 USD Received 20 May 2010; revised 12 Jul 2010; accepted 18 Jul 2010; published 9 Aug 2010

peak position of a noise-ridden signal, it is possible to determine the spread on the calculated peak position: by fitting a Gaussian distribution to the determined peak positions we extract the spread σ. This spread is in turn a measure for the detection limit. Measurements of other structures using our Fourier measurement setup have shown, on average, a signal-to-noise ratio (SNR) of 22 dB. The amplitude of the added noise in the Monte Carlo simulation is therefore chosen as to reach the same SNR.

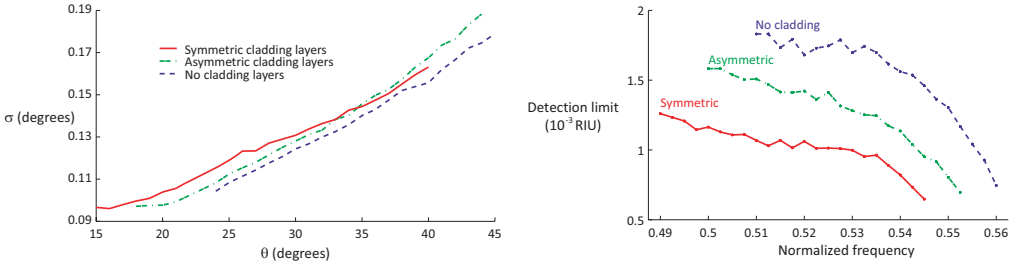

Fig. 6. Adding noise in Monte Carlo simulations delivers the spread σ on correct peak detection (left). The width of the peak, which is in itself dependent on the angle θ, is directly related to this σ. Using this information, we can calculate (right) the detection limit (considering the worst case/largest σ of the shifted peaks). The detection limit is smallest at a high frequency as this is where the peak width is smallest.

Figure 6 leads us to conclude that the spread σ is practically independent of the cladding configuration (variations are due to numerical and statistical errors) but above all, we can say that the spread increases with the angle θ. As already mentioned above, it is therefore interesting to work at a high frequency, which is at small angle θ, close to the normal to the PhC membrane.

Instead of looking at the sensitivity, a more commonly used figure of merit is the detection limit which is defined here as σ/shift. Figure 6 shows the detection limit in function of the frequency for the Fourier setup measurement method. As expected, the detection limit is highest for high frequencies due to the small peak width at these frequencies. If we would be able to increase the SNR of the measurement setup, the detection limit could also improve. Simulations have shown that the detection limit is linearly related to the noise amplitude.

4. Conclusions

Exploiting the coupling of guided to free space modes, we have devised a new photonic crystal based biosensor concept. The major advantage of this device over resonance based sensors (e.g. ring resonators) is that it is able to operate at a single frequency. With a simulated sensitivity of 65° per RIU, the proposed device performs better than a SPR sensor in the angular regime (i.e. operating at a single wavelength) [16]. Furthermore, when fabricating the device there is no need for a metal deposition step or a coupling prism.

If a broadband light source is available, it is possible to operate the device in a reciprocal way by measuring the peak frequency shift at a fixed angle.

Acknowledgments

The author would like to thank imec for providing a research grant. Also gratitude towards K. Van Acoleyen for information on the Fourier setup.

This work was carried out using the Stevin Supercomputer Infrastructure at Ghent University.

#128700 - $15.00 USD Received 20 May 2010; revised 12 Jul 2010; accepted 18 Jul 2010; published 9 Aug 2010

This research was supported by the Interuniversity Attraction Poles program of the Belgian Science Policy Office, under grant IAP P6-10 photonics@be.

#128700 - $15.00 USD Received 20 May 2010; revised 12 Jul 2010; accepted 18 Jul 2010; published 9 Aug 2010